Mapping spatial distribution of soil properties using electrical resistivity on a long term sugarcane trial in South Africa

Gaghik Hovhannissian, Pascal Podwojewski, Yann Le Troquer, Sandile Mthimkhulu, Rianto van Antwerpen

Mapping spatial distribution of soil properties using electrical resistivity on a long term sugarcane trial in South Africa

Gaghik Hovhannissian[1], Pascal Podwojewski[1] Yann Le Troquer[1], Sandile Mthimkhulu[2], Rianto Van Antwerpen[2,3]

[1] IRD, UMR IEES-Paris, SU/IRD/CNRS/INRA/UPEC/Univ. Paris Diderot, Centre IRD de France Nord, 32, Av. H. Varagnat, 93143 Bondy cedex. France

[2]South African Sugar Association Experiment Station, Private Bag X02, Mount Edgecombe, 4300, South Africa

[3]Department of Soil, Crops and Climate Sciences, University of the Free State, PO Box 339, Bloemfontein 9300, South Africa

Abstract

In experimental trials the spatial distribution of soil properties is a key factor to evaluate and determine the credibility of the research outcomes. To evaluate the spatial distribution of soil properties at different depths in the present study, the electrical resistivity method was selected because of its non-destructive nature and high spatial resolution.

The investigation was conducted on BT1 (Burning versus mulching) the world's oldest sugarcane trial (established 25 October 1939) located on the premises of the South African Sugarcane Research Institute (SASRI). The experimental area, covering 7200 m^2, is divided in 32 plots with three crop residue retention treatments. These treatments are either fertilized and not fertilized. The RM15 resistance-meter equipped with a multiplexer was used to collect geophysical data. The latter was used to generate apparent electrical resistivity maps corresponding to three approximate depth ranges: (0 - 0.5 m, 0 - 1.0 m and 0 – 2.0 m). The spatial resolution of the shallowest map (0 - 0.5 m), was 0.5 m x 1.0 m. Bulk density and soil water content, for the 0 - 0.1 m depths, were also determined from samples collected on a grid of 4 m x 5 m. All data collected were georeferenced using a spatial resolution of 4 m x 1 m with the Digital Elevation Model (DEM).

The results of this survey showed the effectiveness of geophysical mapping to reveal detailed information regarding soil spatial variability and to understand and establish the relationships between soil fertility and soil physical properties. Detailed analysis of these results led to the identification of two different soil types on the trial site: a Mollic Cambisol in the upper slope of the trial with a depth of less than 1.0 m and a deeper Mollic Nitisol in the lower slope. Additionally, close to the southern edge of the site, higher values of electrical resistivity

revealed a layer of colluvial deposits, that has not been considered in the past. The relationships between electrical resistivity and investigated soil properties (soil water content, bulk density, aggregate stability and fertilizer) initially seemed paradoxical. Although there is still a need for further investigations, the current study decently establish the rather unexpected relationships. The most striking finding was the high resistivity in fertilised plots associated with the application of potassium chloride fertiliser which led to a decreased soil aggregate stability.

Key words: electrical resistivity mapping, sugarcane, mulch, fertilizer, bulk density, soil water content, soil physical properties, long term trial.

1. Introduction

The current study was conducted in the long-term continuously monitored sugarcane trial (BT1). This trial commenced in October 25, 1939 at the South African Sugarcane Research Institute (SASRI) located in Mount Edgecombe (near Durban) to investigate the effect of greencane harvesting and burning of sugarcane prior to harvest as well as continuous fertiliser application on soil and cane yields (Van Antwerpen et al., 2001). There are several studies that have been conducted in this trial to monitor the changes in soil and crop yield (Van Antwerpen et al., 2001; Graham et al., 2002; Mthimkhulu et al., 2016)..

These studies have revealed that burning of sugarcane prior to harvest under the monocultural system and conventional tillage leads to a decline in soil carbon content (SOC) and soil fertility. Their findings also showed that greencane harvesting, an alternative to pre-harvest burning, encourages the retention and mulching of all leafy non-sucrose containing crop material on the soil surface and potentially increase SOC (Graham et al., 2002). The most recent investigation by Mthimkhulu et al. (2016) reported a significant increase in acidity and a decrease in soil aggregate stability and base cations (calcium and magnesium) which was attributed to mining of nutrients by sugarcane, nitrification and subsequent leaching of base cations. However, none of these studies conducted a precise soil mapping of the trial to provide systematic georeferenced information on the spatial distribution of soil physical characteristics such as depth, texture, bulk density, aggregate stability and soil water properties that might be influenced by the treatments and topography.

Topography is generally one of the major factors in soil formation and its impact is very important on agricultural fields in terms of soil spatial variability, nutrients concentration and leaching of chemicals (mineral fertilizers) and, therefore, has a significant influence on the crop yields (Biggar and Nielsen, 1976; Yang et al., 1998; Iqbal et al., 2005; Senthilkumar et al., 2009). Terrain relative elevation, shape of the relief, slope gradient, as well as its

orientation and its amplitude represent important topographical factors of the soil evolution. They define the principal properties of hydrological functioning of the arable land, like the water flux potential and the peculiarities of the runoff erosion, or sediments transport and deposition (Moore and Burch, 1986; Changere and Lal, 1997; Bakhsh et al., 2000; Kravchenko and Bullock, 2002). Under certain conditions, these phenomena are considered as the main cause of the decline in soil quality on a cultivated steep hillslope (Li and Lindstrom, 2001).

Generally the annual input of organic matter is expected to have a considerable effect on soil porosity, soil structure (Blair, 2000) and soil water content as mentioned by Robertson (2003) but data are scarce. The stability of the aggregates and the connectivity of pores between them is well known to affect the movement and storage of water, aeration, erosion, biological activity and the growth of crops (Amezketa, 1999, Boix-Fayos et al., 2001).

In order to better our understanding of these soil properties and their response to external factors such as topography and land management practices precise mapping is required. Classical approach to mapping soil physical properties is based on data collected at discrete observation points; detailed mapping thus becomes very costly when a large number of data points are required. Opening soil profile pits and sampling large volumes of soil are generally requested for that purpose. However, this *modus operandi* can be very destructive and impossible in an experimental trial covering a relatively small area, and where intensive soil disturbance is unwanted. In this context, the use of geophysical methods has been proven to be efficient and meaningful in the non-intrusive collection of data (Corwin and Lesch, 2003; Samouëlian et al., 2005). As demonstrated in several studies, geophysical techniques, such as electrical resistivity mapping, are very well adapted for use on agronomic trial sites (Corwin and Lesch, 2005; Tabbagh et al., 2000). However an empirical relationship needs to be established for each site between soil electrical resistivity values and soil physical properties

95 as these relationships may be site-specific (Friedman, 2005). Examples of such relationships
96 have been published for water content and bulk density (Cousin et al., 2005), waterlogged soil
97 horizons and spatial-temporal distribution of soil water following irrigation (Michot et al.,
98 2003; McCucheon et al., 2006). Geophysical methods have also been used to study soil
99 textural changes with depth, to evaluate soil thickness *i.e.* the depth to the parent rocks
100 (Milsom, 2003), to locate the presence and to define the thickness of compacted or low
101 density horizons, and to characterise textural properties in duplex soils (McCarter, 1984). It
102 has also been found very efficient in assessing soil salinity through increased electrical
103 conductivity values (Rhoades et al. 1989).
104 To characterize the spatial distribution of the different soil properties in the BT1 experimental
105 site, we applied the method of electrical resistivity mapping with high spatial resolution,
106 corresponding to 3 different depths of investigation.
107 The main objectives of this study were: i.) to collect information on soil spatial variability,
108 soil thickness and pedological changes within the trial, down to approximately 2 m depth; ii.)
109 to analyse and identify changes in electrical resistivity related to soil characteristics, such as
110 water content or bulk density; and, iii.) to assess the impact of different treatments (mulch,
111 fertilization, etc.) on the evolution of soil properties in the experimental plots.

112 **2. Material and methods**

113 *2.1 Site location, soil properties*

114 The experimental site (BT1) is located on the premises of the South African Sugarcane
115 Research Institute, at Mount Edgecombe, in KwaZulu-Natal province, South Africa
116 (31°02'41.10" E ; 29°42'10.82" S). The highest elevation which corresponds to the North-
117 Eastern corner is 99 m above sea level (a.s.l.), with an average slope of 15% facing South-
118 West (Fig.1a). The surface of this experimental site has a parallelogram shape, nearly
119 rectangular, and covers an area of 7200 m² (90 m x 80 m) with the following corner

120 coordinates (36J 310840 E, 6712525 N; 36J310805 E, 6712455 N; 36J310730 E, 6712490 N;
121 36J310765 E, 6712560 N) in the Universal Transverse Mercator (UTM) geographic
122 coordinates system (Fig.1b).
123 The regional climate is subtropical humid and is characterized by summer (October–March)
124 rainfall. The average annual precipitation is 950 mm, and the average annual temperature is
125 20.4°C.
126 The soil was initially classified as Vertisol, (Graham et al. 2002) with a dark (2.5YR 3/1 to
127 3/2) 50 cm thick **A** horizon extending to a dark reddish brown (2.5YR 3/3 to 3/4) AC
128 transitional horizon overlying weathered dolerite. The profile in the upper slope contained a
129 5 cm thick stone-line at a depth of about 30-40 cm overlying weathered dolerite (Fig.2). On
130 the lower slope, the soil has the same A horizon as the upper slope, but overlying a red
131 (2.5YR 3/4 to 10R 3/6) B horizon. The soil texture of the **A** horizon is generally clayey with a
132 little over 40 % of clay and less than 20% of sand in the upper 20 cm. Downstream, in the
133 lower part of the slope, the soil texture becomes clay - loamy with the sand content slightly
134 above 20%. The clay mineralogy is dominated by kaolinite with some scattered evidences of
135 smectite. The soil pH in water is ranging between 4.2 and 5.7. More details of the trial and
136 analytical methods are described by Mthimkhulu et al. (2016).
137 *2.2 Experimental design*
138 This experimental site has been described in details by Thompson (1966), Van Antwerpen
139 and Meyer (1998), and Van Antwerpen et al., (2001). The complete trial is composed of 32
140 plots divided in 4 columns and 8 rows (Fig.1b). Each plot of 175 m^2 is 18 m long and 9.6 m
141 wide. In each plot the sugarcane is planted in 7 rows parallel to the plot long edge and spaced
142 1.37 m. The treatments were: 1) Unburned at harvest with the residue (mainly brown and
143 green leaves) retained on the soil surface to provide a mulch cover (M); 2) Sugarcane burned
144 at harvest with the partially unburned green tops scattered evenly over the soil surface (BS);

145 3) Sugarcane burned at harvest with the unburned green tops removed from the soil surface
146 (BR). These treatments were further subdivided into fertilized (F) and unfertilized plots (F0)
147 in a split-plot design with eight replications for M and four replications for BS and BR
148 treatments.
149 Since the trials' inception in October 25, 1939, the soil at the site has been disturbed only
150 seven times. Initially replanting involved conventional tillage, which imply that the total trial
151 area was ploughed in preparation for planting. In 1970, minimum tillage was adopted with
152 disturbance of the planting row only. All fertilized treatments received 140 kg of nitrogen (N)
153 (as $(NH)_2\ SO_4$ - ammonium sulphate), 28 kg of phosphorus (P) (as P_2O_5 - superphosphate)
154 and 140kg of K (as KCl – potassium chloride) per hectare, applied as 5:1:5 (46%) at 670 kg
155 ha^{-1} approximately 40 days after harvesting (van Antwerpen et al., 2001). There were small
156 fluctuations of the fertilizer composition during the last 20 years. No compensation is made
157 for the nutrients recycled through the retention of residue after harvest. Since 1987 the crop is
158 annually harvested in spring (September) at the beginning of the rainy season.
159 It may be added that the presence of termite nests of *Odontotermes sp.* was evidenced by
160 vertical chimneys deeper than 0.6 m and with a diameter of 0.15 m at the north of plot 9 and
161 west of plot 22 (Fig. 1b). In that area, termite nests are generally located on the external
162 border of sugarcane plot surrounded by grass pathways.
163 *2.3 Topographic survey*
164 A high precision topographic map of the study area was created using a laser tacheometer
165 (LEICA Total Station - TC 302). The use of this equipment made it possible to determine the
166 horizontal coordinates (X and Y) with errors less than ± 0.10 m, and the altitude Z, with errors
167 smaller than ± 0.05 m.
168 This survey was carried out for two reasons: (i) in order to be able to study the impact of
169 topography on soil properties at large; (ii) and to define the georeferenced coordinates of each

plot and their boundaries with high precision. For the elevation model, the measurements over the entire site were made at the nodes of a 4 m x 1 m rectangular grid. A 0.5 m mesh digital elevation model (DEM) was generated using these results, which provides the accuracy and density of measurement points required. Thanks to this model, all actions and experimental interventions (positions of different sensors, auger soundings or pedological pits, etc.) could be now georeferenced.

2.4 Soil water content and bulk density

The soil samples used for the determination of soil water content (SW) and bulk density (BD) were collected from the whole trial area at the 0–10 cm soil layer, following a 4 m x 5 m grid. This sampling was made simultaneously with measurements of electrical resistivity. A total of 325 undisturbed soil cores (250 cm^3) were collected: 275 within the plots and 50 within the alleys. All the samples were oven dried at 105°C for 24 hours. The final results will be presented as two maps (SW and BR) where the "Nearest Neighbour" data interpolation method has been used for both parameters.

2.5 Soil structural stability

The soil structural stability was determined on the soil samples using the fast wetting AFNOR (2005) method developed by Le Bissonais (1996). The aggregate stability data, calculated from a nest of six sieves (2, 1, 0.5, 0.2, 0.1 and 0.05 mm), was converted to mean weight diameter (MWD) according to Kemper and Rosenau (1986). Three replicate soil samples used to measure this parameter were collected at two depths (0-10 and 10-20 cm, i.e. six samples per plot) from three mini-pits in each of the thirty-two plots. The total of samples analysed for MWD was 192.

2.6 Apparent electrical resistivity mapping

Electrical resistivity mapping of the whole trial, including breaks between plots, was carried out in November 2011, after harvesting that took place in September, but prior to the annual

195 fertilization.

196 For the measurements we used the so called "pole-pole" configuration of electrodes,
197 consisting of two mobile electrodes (the current electrode and the potential electrode) with the
198 second pair (current and potential) of electrodes remote and fixed far enough from the
199 prospecting area, to be considered as an infinite distance. This condition is satisfied if the
200 remote electrodes are placed at a distance greater than 20 times the spacing between the
201 mobile electrodes (Robain et al., 1999). The use of the "pole-pole" electrode array is justified
202 because it reduces the number of mobile electrodes from 4 to 2 for each measurement, and
203 thus allow high productivity. This electrode configuration is relatively sensitive to non-
204 horizontal boundaries and heterogeneities and provides greater depths of investigation,
205 compared to other arrays (Seaton and Burbey, 2002). At the surface of a homogeneous
206 medium, it measures the so-called “true resistivity” of the medium (ρ) (expressed in Ohm·m
207 or Ω·m). It integrates a volume of medium roughly hemispheric around the 2 mobile
208 electrodes, *i.e.* down to a depth roughly equal to the electrode spacing (Oldenburg and Li,
209 1999). At the surface of a non-homogeneous environment, in the case of our survey for
210 instance, the equipotential surfaces around the current electrode are no more hemispheric;
211 their actual geometry depends on the different media around the electrodes; it measures a so-
212 called “apparent resistivity” (ρ_a) *(*expressed also in Ohm·m or Ω·m), related to the true
213 resistivities of the surrounding media. Practical experience and numerical modelling however
214 have proven that: (i) the greater the separation between the two electrodes, the greater the
215 depth of exploration and (ii) apparent resistivity maps can be interpreted qualitatively and
216 provide very useful information on the study site. Inversion procedures to transform apparent
217 resistivities into 2 or 3 dimensional models with “true resistivities”, so-called “electrical
218 tomographies”, require much heavier and costly field operations, which are performed only
219 when detailed investigations and modelling are mandatory.

220 The measurements were performed using a "Resistance Meter RM-15" equipped with a
221 "MPX15 multiplexer" and connected to a "PA20 multi-probe array" (Geoscan Research,
222 Heather Brae, Chrisharben Park, Clayton, Bradford, West YorkshireBD14 6AE, UK).
223 To simplify the transportability of the instrument by a single operator from one point of
224 measurement to the next, the resistance-meter and the multiplexer are fixed on a versatile
225 frame whose basis is a beam with a length of 2 m, on which 5 stainless steel electrodes are
226 mounted with a spacing **a** = 0.5 m. During mapping, the measurements were carried out
227 moving the device forward with 1 m intervals along lines perpendicular to the northern edge,
228 and with 2 m spacing between successive lines. Seven readings were recorded at each
229 position of the device: 4 measurements with an electrode spacing of 0.5 m (**a** = 0.5 m); two
230 measurements with electrode spacing of 1.0 m (**a** = 1.0 m) and one measurement with
231 electrode spacing of 2.0 m (**a** = 2.0 m). The number of measurements obtained with a
232 0.5 m x 1.0 m 1.0 m x1.0 m, and 2.0 m x 1.0 m grid spacing were 13600; 6800 and 3400 data
233 points respectively. We were thus able to draw and present three “apparent resistivity” maps
234 representative of three soil thicknesses, approximately 0 - 0.5 m, 0 – 1 m and 0 – 2 m.
235 These maps were analysed by comparison with the topographic features, water content, bulk
236 density, and aggregate stability characteristics, at the relevant depths (0 – 10 cm and 10 –
237 20 cm).

238 **3. Results**

239 *3.1 Topographic survey*

240 From our topographic survey, as mentioned above (§2.3), a 0.5 m mesh Digital Elevation
241 Model (DEM) was generated. This model was used to determine slope gradients and other
242 specific relief features were determined, as shown on Fig. 3. The highest absolute elevation
243 was equal to 99 m a.s.l., while the lowest was 85 m a.s.l., isohypses every 0.5 m altitude
244 difference, magnitude and azimuth of slope gradients as shown by vectors.

245 The surface of the trial is mainly facing southwest with the axis of the general slope
246 coinciding approximately with the NE-SW diagonal. The average slope along this axis is
247 12 %, but it is not constant. It represents a convex then concave shape, with an average slope
248 of 10-12 % close to the upper northeast corner; in the central part of the trial, the slope
249 increases to 15-17 %, and then declines to 4-8 % at about 15-20 meters, near the southwest
250 corner. The difference in altitude is larger at the eastern (10.5m) and northern edges (9.2 m),
251 compared to the western (4.6 m) and southern edges (3.2 m). In addition, these slopes are
252 neither uniform nor linear. So, it should however be noted that the topographic surface of the
253 trial is rather complex and this can have major impacts on the soil properties.
254 On the map (Fig.3), the arrows indicate the energy and direction of the rainwater flows. They
255 exhibit rather large differences in magnitude and azimuths: the flow direction is a)
256 approximately perpendicular to the sugarcane rows in the eastern part of the site, b), it crosses
257 the rows with an angle close to 45° in the central and south-western parts, and c) it is
258 practically parallel to the rows in the north-western part. These important differences in
259 intensity and direction of the water flows are major features of the trial site because of their
260 substantial influence on the erosion and dissolution phenomena, as well as on the transport
261 and deposition of solutes and suspended particles.
262 *3.2 Soil water content and bulk density*
263 The main SW results are shown on Fig. 4a and 4b. The points in Fig.4a indicate the positions
264 where soil samples used for SW and the BD (bulk density) values were collected. The map of
265 SW determined at 0-10 cm, indicated that this property is affected by crop residues retention
266 treatment (i.e. M treatments show high values of SW).
267 The SW increased with increase in crop residues on the soil surface in fertilized and
268 unfertilized treatments as anticipated (0.36 $kg \cdot kg^{-1}$ for (MF) plots >BSF (0.24 $kg \cdot kg^{-1}$) > BRF
269 (0.19 $kg \cdot kg^{-1}$) and MF0 (0.32 $kg \cdot kg^{-1}$) > BSF0 (0.25 $kg \cdot kg^{-1}$ > BRF0 (0.20 $kg \cdot kg^{-1}$) (Fig. 4b).

The SW median values in MF treatment (0.36 $kg \cdot kg^{-1}$) are slightly higher compared to the MF0 treatment (0.32 $kg \cdot kg^{-1}$), and this could be attributed to the larger amount of residue material resulting from the combination of fertilizer and crop residues. The SW differences are observed between the fertilized and unfertilized plots were not significant for BS and BR treatments. Concerning the dispersion, *i.e*. the distance between the two extreme quartiles, it is rather small for BR and BS and greater at the M treatment.

Similarly to the SW map, with the soil bulk density (BD) map, all the M treatments were easy to identify (Fig.5a), The highest and the lowest bulk densities were measured at BR (1.18 $g \cdot cm^{-3}$) and M treatments (0.82 $g \cdot cm^{-3}$) respectively. The same statistical approach as above has been applied to each six populations (Fig.5b). The general trend showed a decrease in BD from 1.13 $g \cdot cm^{-3}$ at BRF0 to 1.0 $g \cdot cm^{-3}$ at the MF. Fertilized plots had lower BD values across all the crop residue treatments compared to F0. Besides the measurements are characterized by relatively high interquartile dispersions, indicating large heterogeneities in the density the investigated soil.

3.3 Soil structural stability (MWD)

The MWD are presented in Fig.6a and 6b, These results indicated that the MWD does not vary much relative to the residue treatments, but it decreased significantly in the F plots in both mulched and burnt treatments. The MWD in F0 ranged from 1.72 mm (BSF0) to 2.33 mm (BRF0) at 0 – 10 cm depths, and from 2.22 mm (MF0) to 2.41 mm (BRF0) at 10 – 20 cm depths.

It was also worth noting that MWD were slightly higher at 10 – 20 cm depths of F treatment, the median values ranging from 1.50 mm for MF to 1.75 mm for BRF, and from 1.11 mm for BRF to 1.37 mm for MF. at 0 – 10 cm depths. An increase in MWD (from 1.11 in BRF to 1.37 mm in MF) attributed to increase in crop residues was only observed at 0 – 10 cm of the F treatment. At 10 – 20 cm depths, it decreased, from 1.75 mm to 1.50 mm.

295 The results also show that the fertilizer application leads to a nearly identical light decrease in
296 MWD values, from 0.6 mm to 0.8 mm, for all types of treatments at both depths, except for
297 the difference between (BRF0) and (BRF) at 0 – 10 cm depths, where it is quite large
298 (1.22mm), representing a variation greater than 50%.

299 *3.4 Soil electrical resistivity mapping*

300 Three apparent electrical resistivity (ρ_a) maps are shown on Fig.7 a, b and c, corresponding to
301 three increasing thicknesses, as explained above, since they represent the results of
302 measurements with increasing electrode spacing **a**, from 0.5 m to 1.0 m and to 2.0 m.

303 The map representing the measurements with electrode spacing **a** = 0.5 m (Fig.7a) should be
304 the most sensitive to the soil properties, since it corresponds to the shallowest depth of
305 investigation. In the central part of this map, a band of low resistivity values (roughly
306 $\rho_a \leq 20$ Ohm·m) is observed, extending from the north-western to the south-eastern corner.
307 The boundaries of this zone are almost parallel to the topography.

308 Within this area the seven plots that seem to be more conductive than others include:
309 1 (BSF0), 2 (BRF), 4 (BRF0), 11 (MF0), 13 (BRF0), 20 (MF0) and 32 (MF0); It is worth
310 noting that about 85% of these samples are F0 and that there were only three plots in the F
311 treatments that showed slightly more resistivity, namely; 3 (BSF), 12 (MF) and 22 (BSF).
312 Moreover, the highest values of apparent resistivity ($\rho_a > 25$ Ohm·m) were found in the
313 northeast of the central conductive area.Three out of the four southern plots show relatively
314 high resistivity values, around 30 – 35 Ohm·m.

315 The map corresponding to **a** = 1.0 m (Fig. 7b), the intermediate thicknesses, shows a similar
316 pattern as Fig. 7a. The central conductive strip appears sharper and more homogeneous,
317 especially to the west. The north-eastern resistive area looks also more homogeneous and its
318 southern boundary follows isohypses very well. Compared to the previous map, the southern
319 resistive area is reduced in intensity and dimensions.

320 The third map (**a** = 2 m) (Fig. 7c), with the greatest depth of investigation, shows a regular
321 gradient from the northeast to the southwest, following the isohypses. The resistivity values
322 decrease from about 40 Ohm·m down to approximately 15 Ohm·m.
323 It is important to note that as soon as these 3 maps were available, *i.e*. during the survey, 17
324 points were selected from the entire surface of the BT 1 trial, where auger drillings were
325 performed to establish the relationship between the electrical resistivity distribution and
326 various soil properties, such as its nature, thickness, texture, soil aggregate stability, SW and
327 BD.
328 These 3 maps definitely allowed us to characterize the spatial variability of the soil properties
329 of the trial. First, these results have assisted in the reclassification of soils of the trial and also
330 formed basis of the further studies. For instance, this this trial was believed to have one soil
331 type known as Vertisol. However, the current study showed there are two soils in this trial
332 which are: Mollic Cambisol to the Northeast and Mollic Nitisol to the South- and Southwest
333 (Mthimkhulu et al., 2016).
334 **4. Discussion**
335 The outcomes of the electrical resistivity mapping of the trial provided four types of
336 information: (i) variation of the soil thickness in relation to topography, which further led to
337 the with two different soil types separated by altitude; ii) Existence of a soil thin layer of
338 colluvium origin, located in the lower part of the trial; iii) Land management influence on soil
339 properties.
340 *i.) Soil thickness*
341 The electrical resistivity (ρ_a) map with the greater depth of investigation (Fig. 7c) shows a
342 high resistivity anomaly in the North-East part, and good correlation with topography. It is
343 enhanced on Fig.8b obtained through low pass filtering of the raw map (a=2m). These results
344 could be due to the closeness of soil surface to the parent rock as a result of shallow depth (<

345 1 m). The depth of the parent rock was confirmed soil auguring, which additionally led to the
346 reclassification of the soil trial. The soil of the entire trial was initially classified as a Vertisol.
347 For this upper part of trial, it is now re-classified as a Mollic Cambisol (IUSS Working Group
348 WRB, 2014), with a thick well-structured dark AB horizon, directly laying on the weathered
349 dolerite. The deep soil in the South and South Western parts of trial is now classified as a
350 Mollic Nitisol with a dark reddish B horizon (Mthimkhulu et al., 2016). The limit between the
351 two soil types, after Mthimkhulu et al. (2016), is shown on the map (Fig. 8b); it could be
352 better ascertained through additional soundings. It should also be noted that in plots 27 and
353 28, dolerite stones are visible on the surface, and the thickness of the soil does not exceed
354 0.5 m.
355 *ii.) Superficial colluvial layer*
356 The electrical resistivity map with (a=0.5 m) the shallowest depth of investigation (Fig. 7a)
357 shows a high resistivity anomaly to the South-West of the trial, which gradually decreases its
358 intensity and extension on the other two maps (Fig. 7b and c) with deeper depths of
359 investigation. It has been proven through augering the soundings and by further physical
360 analysis of the samples that it is due to the presence of a colluvial layer, with higher sand
361 content (Mthimkhulu et al., 2016). Downstream, where the soil has clay loam texture, the
362 sand content is slightly over 20 % only in plots 8 (MF), 16 (BSF0) and 24 (BRF), and this
363 fraction is less than 20% in all other plots. This is also confirmed by the higher BD values on
364 the same plots 8, 16 and 24. The existence of colluvial deposits had never been detected prior
365 to electrical resistivity mapping. It appears to be, as a matter of fact, directly related to the
366 features of the relief.
367 *Land-management effects on electric resistivity*
368 The two maps (SW) and (BD) maps (Fig. 4a and Fig. 5a) showed a clear response to residue
369 treatments: i.e. higher water content and lower bulk density in the M plots, versus lower water

content and higher bulk density in the BR plots and intermediate values in the BS plots. From classical scientific literature and our experience, we expected a clear and robust relationship between SW and the electrical resistivity, especially on the map corresponding to the shallowest depth of investigation (Fig. 7a). This anticipation emanated from that SW has a sensitivity to the changes that occur in other soil properties and land management practices. This map, as mentioned above, appears to be strongly influenced by the resistive anomalies related to the thickness of soil and the colluvial layer although, and no obvious consistency appears with the water content at first glance. Thorough analyses of Figure 7a showed that virtually all fertilized plots, except for plot 2, are fully or partially characterized by relatively higher electrical resistivity values compared to the unfertilized treatments. This appears as a major paradox: high electrical resistivity values are observed in the plots with higher water content and, furthermore, these plots have received an additional mineralization.

The relationship between electrical resistivity and soil properties in this trial appears to be more complex than expected. Would that be a general rule in soil sciences?

According to Archie's law,, electrical resistivity of porous consolidated media decreases with increasing SW and mineralisation (Glover et al., 2000). Some results concerning soil studies tend to prove that a somewhat similar law may apply (Michot et al., 2003, McCucheon et al. 2006). According to Cousin et al., (2005) however, the relationship between the electrical resistivity and water content is not so simple, as they showed that electrical resistivity decreases with increase in BD. This may partly of the reasons for the observed high electrical resistivity values in fertilized plots accompanied by a decrease of BD in the current study.

These observations could be due to chemical reactions occurring in the soil.. On the one hand, fertilizers application increases the concentration of ions in the soil which results raises the electrical conductivity of the soil, especially in plots regularly fertilized with potassium chloride (KCl) (Rhoades et al., 1999). On the other hand, changes in the chemical

composition and ion concentration of the soil affect its equilibrium and may lead to physicochemical interactions influencing soil aggregation, namely the degradation of soil structural stability.

In a recent publication Paradelo et al. (2013) reported a severe clay dispersion resulting from the application of different forms of KCl and soil acidification (with however no dispersion) where NH^{4+} was applied in a 48 experimental plots located in Versailles. The dispersive effect of K^{+} on clays was confirmed by several studies conducted by Marchuk and Rengasamy (2012). In contrast, the study of Van Antwerpen and Meyer (1998) conducted at BT1 trial concluded that K^{+} did not cause dispersion due to the release of Al under the low pH conditions. From the same experimental site, Graham et al. (2002) noticed a slight increase in both exchangeable and non-exchangeable K^{+} content in the mulched treatment. The major difference recently measured (at BT1) between the different treatments was the significant decrease of divalent exchangeable cations Ca^{++} and Mg^{++} in fertilized plots concomitant with a decrease of pH (Mthimkhulu et al., 2016).

For these last three studies mentioned above, conducted at different years on the BT1 trial, the samples were collected between January and March, which is the time coinciding with the sugarcane growth period. Ion concentrations measured on soil samples collected from the fertilized plots can be relatively higher compared to those in November when electrical resistivity mapping was performed, since nutrients are continuously extracted until the crop is harvested in September or October.

It could also be assumed that fertilizers can be dissolved and leached by rain, since the rainy season begins around August, with a monthly average of 70 mm, reaching its maximum of approximately 120mm in November.

With these observations it could be deduced that the high electrical resistivity values systematically observed in the fertilized plots with chemical inputs (Fig. 6a and b) are due to

420 the soil structural stability degradation, related to complex physicochemical interactions. This
421 deduction is also in agreement with the influence of the so-called pore tortuosity. The
422 tortuosity factor is known to be important in contributing to high resistivity in porous media
423 (Kunetz, 1966). While this factor was well documented for rocks and reconstructed porous
424 media, it is not yet considered for soils and inter-aggregate porosity.
425 To conclude, we believe that a better understanding of the origin of these high electrical
426 resistivity values in the fertilized plots, requires additional experimental and theoretical work.
427 *The presence of termite nests*
428 The termites of the *Odontotermes sp.* specie are a fungus-culturing termites, making comb
429 nest chambers with large void space that could generate high values of local electric
430 resistivity (Fig. 7a). However, the decrease in the resolution of the measurement with depth
431 make it difficult to separate resistivity features of termite nests from other sources, resulting
432 in high resistivity.
433 **Conclusion**
434 The results of electrical resistivity mapping of the investigated trial showed strong lateral
435 variations associated to the soil thickness, soil texture and other soil properties. The main
436 findings were as follows: i) Soil depth increased from North East to the South West of the
437 trial , but this had no effect the on topsoil characteristics (0-20 cm). This study revealed that
438 the trial was established on two different soils including Cambisol (upper slope) and Nitisol
439 (lower slope) although previous studies have reported a single soil type (Vertisol) in this trial;
440 ii) The increase in soil resistivity and depth in the SW corner of the trial was attributed to
441 accumulation of colluvium material; it may now be considered as a possible hidden limiting
442 factor for sugar cane growth apart from the sole treatment effect, and be included in further
443 investigations of yield variability ; iii). The soil resistivity in the soil surface showed no clear
444 relationship with SW content or bulk density (mulch effect) and this was found to be very

445 strange as SW was significantly higher in the topsoil of M plots; iv). The topsoil resistivity
446 showed some relationship with fertilizer treatments such that higher electrical resistivity
447 observed in fertilized plots was associated with lower soil structural stability measured in the
448 treatment. However the electric resistivity was not related to the inputs of salts (KCl) as
449 fertilizers; v) The termite nests are identified to be more resistant but no correlation with
450 resistant points and termite nests could be established.
451 The results of the soil electrical resistivity mapping showed that the effect of long term use of
452 fertilizers deeply affects the porous media and soil physical properties, while mulching only
453 temporarily affects the soil surface water content and bulk density, with limited effects on the
454 soil structural and chemical properties at depth.
455 Geophysical mapping appear as time-consuming and as a relatively heavy operation, but the
456 information it provides makes it largely beneficial, from a methodological, as well as from a
457 practical point of view. However, having reported that, further experimental and theoretical
458 works are still needed to better understand the relationship between electrical resistivity and
459 all classical pedological parameters. The current experimental survey provided an
460 instantaneous pictorial representation of soil variability that was required for the better
461 understanding of the interaction of factors and processes leading to the evolution of this long-
462 term trial.
463

464 References

465 AFNOR NF X31-515., 2005. Mesure de la stabilité d'agrégats de sols pour l'évaluation de la
466 sensibilité à la battance et à l'érosion hydrique, AFNOR, Paris, mars 2005. 13p.
467 Amezketa, E., 1999. Soil aggregate stability: a review. J. of Sustainable Agric. 14, 83-151.
468 Bakhsh, A., Colvin, T.S., Jaynes, D.B., Kanwar R.S., Tim U.S., 2000. Using soil attributes
469 and GIS for interpretation of spatial variability in yield. Trans. ASAE 43, 819–828.
470 Biggar, J. W., Nielsen, D. R., 1976. Spatial Variability of the Leaching Characteristics of a
471 Field Soil. Water Resour. Res. 12, 78-84.
472 Blair, N., 2000. "Impact of cultivation and sugar-cane green trash management on carbon
473 fractions and aggregate stability for a Chromic Luvisol in Queensland, Australia." Soil &
474 Till. Res. 55, 183-191.
475 Boix-Fayos, C., Calvo-Cases, A., Imeson, A.C., 2001. Influence of soil properties on the
476 aggregation of some Mediterranean soils and the use of aggregate size and stability as
477 land degradation indicators. Catena. 44, 47-67. DOI: 10.1016/S0341-8162(00)00176-4
478 Changere, A., and Lal. R., 1997. Slope position and erosional effects on soil properties and
479 corn production on a Mianian soil in central Ohio. J. Sustain. Agric. 11, 5–21.
480 Corwin, D.L., Lesch, S.M., 2003. Application of soil electrical conductivity to precision
481 agriculture: theory, principles, and guidelines. Agron. J. 95, 455–471.
482 Corwin, D.L., Lesch, S.M., 2005. Apparent soil electrical conductivity measurements in
483 agriculture. Comput. Electron Agr. 46, 11–43
484 Cousin, I., Besson, A., Aboubacar Sani, A., Accart, V., Samouëlian, A., Cornu, S., Richard,
485 G., 2005. Influence of soil water content, soil bulk density, soil solution composition on
486 electrical resistivity measurements. EGU 05 Geophys. Res. Abstracts 7, 08150.
487 Friedman, S.P., 2005. Soil properties influencing apparent electrical conductivity: A review.
488 Comput. Electron. Agric. 46, 45 – 70.

Glover, P.W.J., Hole, P. J., Pous, J., 2000. A modified Archie's law for two conducting phases. Earth Plan. Sci. Let. 180 (3 _ 4), 369 – 383.

Graham, M.H., Haynes, R.J., Van Antwerpen, R., 2002. Size and activity of the soil microbial biomass in the row and interrow of a sugarcane field under burning and green cane harvesting. Proc. S. Afr. Sug. Technol. Assoc. 76, 186-195.

Iqbal, J., Read, J. J., Thomasson, A. J., Jenkins J. N., 2005. Relationships between Soil–Landscape and Dryland Cotton Lint Yield. Soil Sci. Soc. Am. J. 69, 872–882.

IUSS Working Group WRB., 2014. World Reference Base for Soil Resources 2014. International soil classification system for naming soils and creating legends for soil maps. World Soil Resources Reports No. 106. FAO, Rome.

Kemper, W.D., Rosenau, R.C., 1986. Aggregate stability and size distribution. In: A. Klute (Ed.), Methods of Soil Analysis: Part 1, Physical and Mineralogical Methods, 2nd Agronomy Monograph No 9, Book Series 5, Soil Sci. Soc. of Am., Madison, WI, 425–442.

Kravchenko, A.N., Bulloc, D.G., 2002. Spatial variability of soybean quality data as a function of field topography: I. Spatial data analysis. Crop Sci. 42, 804 – 815.

Kunetz, G., 1966. Principles of direct current resistivity processing. Gebruder Borntraeger.

Le Bissonnais, Y., 1996. Aggregate stability and assessment of soil erodibility: I. Theory and methodology. Eur. J. Soil Sci. 47, 425-437.

Li, Y., Lindstrom, M.J., 2001. Evaluating soil quality–soil redistribution relationship on terraces and steep hillslope. Soil Sci. Soc. Am. J. 65, 1500–1508.

Marchuk, A., Rengasamy, P., 2012. Threshold electrolyte concentration and dispersive potential in relation to CROSS in dispersive soils. Soil Res. 50(6), 473-481. http://dx.doi.org/10.1071/SR12135

McCarter, W.J., 1984. The electrical resistivity characteristics of compacted clays.

514 Géotechnique. 34, 263–267.
515 McCutcheon, M.C., Farahani, H.J., Stednick, J.D., Buchleiter, G.W., Green, T.R., 2006.
516 Effect of soil water on apparent soil electrical conductivity and texture relationships in a
517 dryland field. Biosyst. Eng. 94, 19–32.
518 Michot, D., Benderitter, Y., Dorigny, A., Nicoullaud, B., King, D., Tabbagh, A., 2003. Spatial
519 and temporal monitoring of soil water content with an irrigated corn crop cover using
520 electrical resistivity tomography. Water Resour. Res. 39, 11-38.
521 Milsom J., 2003. Field Geophysics. 3rd Edition, John Wiley & Sons, New York, 244.
522 Moore, I.D., Burch, G.J., 1986. Physical basis of length-slope factor in the universal soil loss
523 equation. Soil Sci. Soc. Am. J. 50:1294 – 1298.
524 Mthimkhulu, S., Podwojewski, P., Hughes , J., Titshall , L., Van Antwerpen, R., 2016. The
525 effect of 72 years of sugarcane residues and fertilizer management on soil physico-
526 chemical properties. Agric. Ecosyst. Environ.. 225, 54-61.
527 Mualem, Y., Friedman, S., 1991. Theoretical prediction of electrical conductivity in saturated
528 and unsaturated soil. Water Resour. Res. 27, 2771–2777. DOI: 10.1029/91WR01095.
529 Oldenburg, D.W., Li, Y., 1999. Estimating depth of investigation in DC resistivity and IP
530 surveys. Geophysics. 64 (2), 403–416.
531 Paradelo, R., van Oort, F., Chenu, C., 2013. Water-dispersible clay in bare fallow soils after
532 80 years of continuous fertilizer addition Geoderma. 200-201, 40-44.
533 Rhoades, J.D., Manteghi, N.A., Shouse, P.J., Alves, W.J., 1989. Soil electrical conductivity
534 and soil salinity: new formulations and calibrations. Soil Sci. Soc. Am. J. 53, 433–439.
535 Rhoades, J. D., Chanduvi, F., Lesch, S., 1999. Soil salinity assessment: Methods and
536 interpretation of electrical conductivity measurements. Irrigation and drainage paper,
537 N° 57, 165. FAO, Rome.
538 Robain, H., Albouy, Y., Dabas, M., Descloitres, M., Camerlynck, Ch., Mechler, P., Tabbagh,

539 A., 1999. The location of infinite electrodes in pole – pole electrical surveys:
540 consequences for 2D imaging. J Appl. Geophys. 41, 313 – 333.
541 Robertson, F., 2003. Sugarcane Trash Management: Consequences for Soil Carbon and
542 Nitrogen – Final Report of the Project Nutrient Cycling in Relation to Trash
543 Management. CRC Sugar Technical Publication. CRC for Sustainable Sugar Production,
544 Townsville.
545 Samouëlian, A., Cousin, I., Tabbagh, A., Bruand, A., Richard, G., 2005. Electrical resistivity
546 survey in soil science: a review. Soil Till. Res. 83, 173-193.
547 Seaton, W., Burbey, T.J., 2002. Evaluation of two-dimensional resistivity methods in a
548 fractured crystalline-rock terrane. J. Appl Geophys. 51 (1), 21–41.
549 Senthilkumar, S., Kravchenko, A.N., Robertson, G.P., 2009. Topography influences
550 management system effects on total soil carbon and nitrogen. Soil Sci. Soc. of Am. J. 73,
551 2059–2067.
552 Tabbagh, A., Dabas, M., Hesse, A., Panissod C., 2000. Soil resistivity: a non-invasive tool to
553 map soil structure horizonation. Geoderma 97, 393–404.
554 Thompson, G.D., 1966. The production of trash and its effect as a mulch on the soil and on
555 sugarcane nutrition. Proc. S. Afr. Sug. Technol. Assoc. 40, 333-342.
556 Van Antwerpen, R., Meyer, J.H., 1998. Soil degradation II: Effects of trash and inorganic
557 fertilizer on soil strength. Proc. S. Afr. Sug. Technol. Assoc. 72, 152-158.
558 Van Antwerpen, R., Meyer, J.H., Turner, P.E.T., 2001. The effects of cane trash on yield and
559 nutrition from the long-term field trial at Mount Edgecombe. Proc. S. Afr. Sug. Technol.
560 Assoc. 75, 235–241.
561 Yang, C., Peterson, C.L. Shropshire, G.J., Otawa T., 1998. Spatial variability of field
562 topography and wheat yield in the Palouse region of the Pacific Northwest. Trans. ASAE.
563 41, 17–27.
564

565 **Captions and figures**

566 Figure 1a. An aerial view of BT1 trial, with reference to geographical coordinates.

567 Figure 1b. Schematic view of the experimental site BT 1: 32 plots, 3 types of treatments (BR,
568 BS and M), split between fertilized (F) and unfertilized (F0).

569 Figure 2. Profile of a Mollic Cambisol located 10 m East of plot 27.

570 Figure 3. Topographic map and slope gradient vectors: 0.5 m isohypse intervals.

571 Figure 4a. Map of Soil Water Content (SW), overlaid to topography and to the positions of
572 the collected and analysed samples

573 Figure 4b. Results of SW measurements with box and whiskers,

574 Figure 5a. Map of Bulk Density (BD), overlaid to topography.

575 Figure 5b. Results of BD analysis

576 Figure 6a. Results of Mean Weight Diameter (MWD), expressed in mm, for the samples
577 collected in the 0 – 10 cm depth range.

578 Figure 6b. Results of statistical analysis of Mean Weight Diameter (MWD), expressed in mm,
579 for the samples collected in the 10 – 20 cm depth range.

580 Figure 7a. Electrical apparent resistivity (ρ_a) map, expressed in Ohm·m (Ω·m) for electrode
581 separation **a** = 0.5 m.

582 Figure 7b. Electrical apparent resistivity (ρ_a) map, expressed in Ohm·m (Ω·m) for electrode
583 separation **a** = 1 m.

584 Figure 7c. Electrical apparent resistivity (ρ_a) map, expressed in Ohm·m (Ω·m) for electrode
585 separation **a** = 2 m.

Figure 8. Low-pass filtered electrical apparent resistivity (ρ_a) map, expressed in Ohm·m (Ω·m) for electrode separation **a** = 2 m, showing additionally the boundary separating the 2 types of soil to the NE (continuous line) and the limit of the colluvial deposits to the SW (dashed line).

Figure 1a

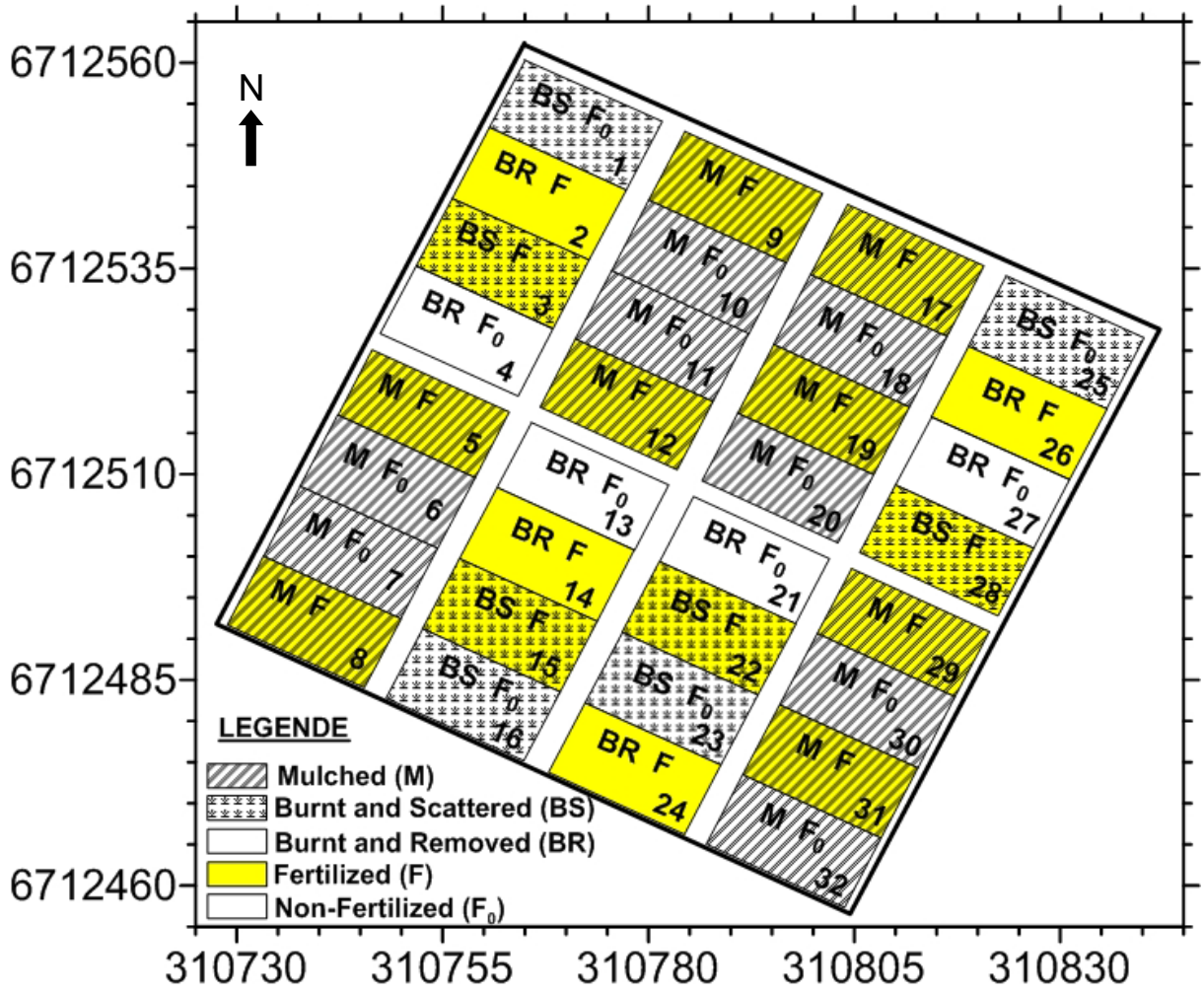
6712560
6712535
6712510
6712485
6712460
310730
310755
310780
310805
310830
N
BS F0 1
BR F 2
BS F 3
BR F0 4
M F 5
M F0 6
M F0 7
M F 8
M F 9
M F0 10
M F0 11
M F 12
BR F0 13
BR F 14
BS F 15
BS F0 16
M F 17
M F0 18
M F 19
M F0 20
BR F0 21
BS F 22
BS F0 23
BR F 24
BS F0 25
BR F 26
BR F0 27
BS F 28
M F 29
M F0 30
M F 31
M F0 32
LEGENDE
Mulched (M)
Burnt and Scattered (BS)
Burnt and Removed (BR)
Fertilized (F)
Non-Fertilized (F0)

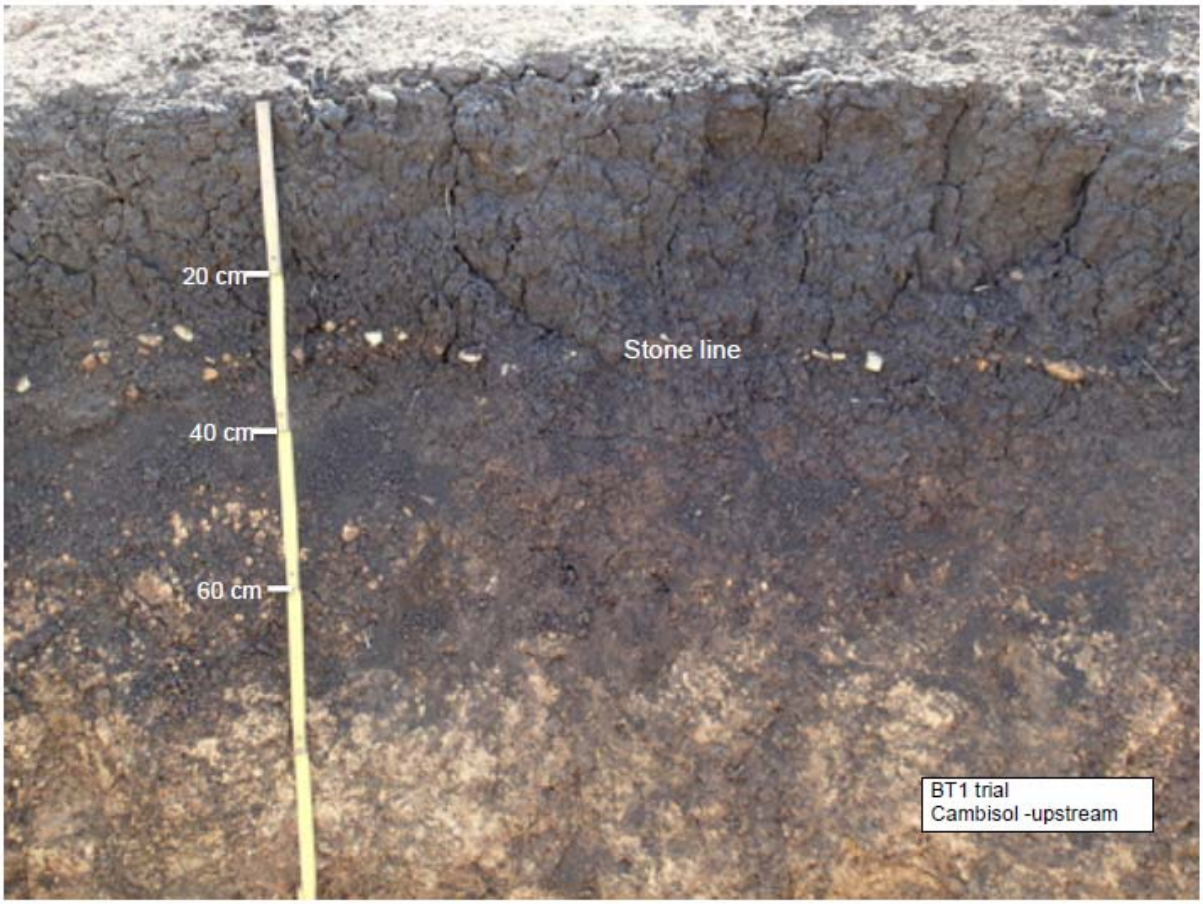

Figure 2

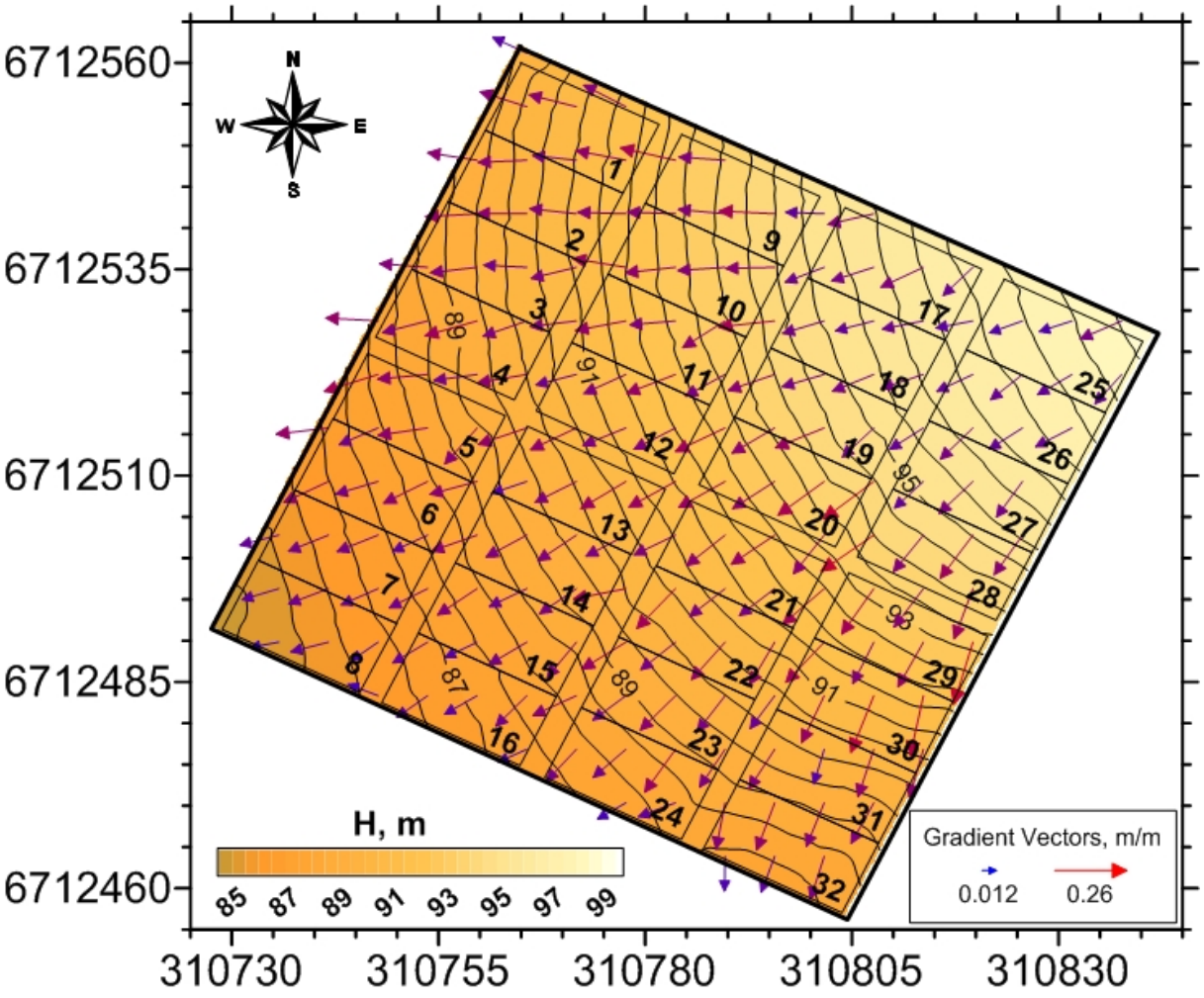
6712560
6712535
6712510
6712485
6712460
310730
310755
310780
310805
310830
N
W
E
S
H, m
85
87
89
91
93
95
97
99
Gradient Vectors, m/m
0.012
0.26

Figure 3

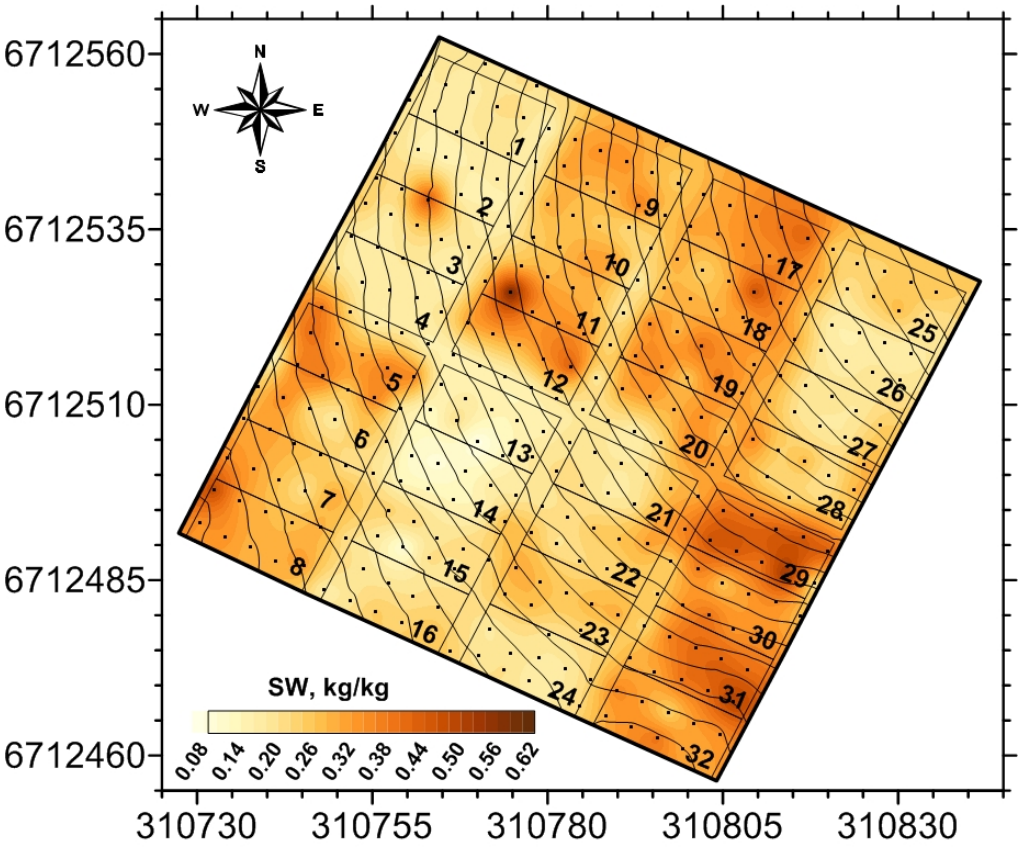
6712560
6712535
6712510
6712485
6712460
310730
310755
310780
310805
310830
N
W
E
S
SW, kg/kg
0.08
0.14
0.20
0.26
0.32
0.38
0.44
0.50
0.56
0.62
1
2
3
4
5
6
7
8
9
10
11
12
13
14
15
16
17
18
19
20
21
22
23
24
25
26
27
28
29
30
31
32

Figure 4a

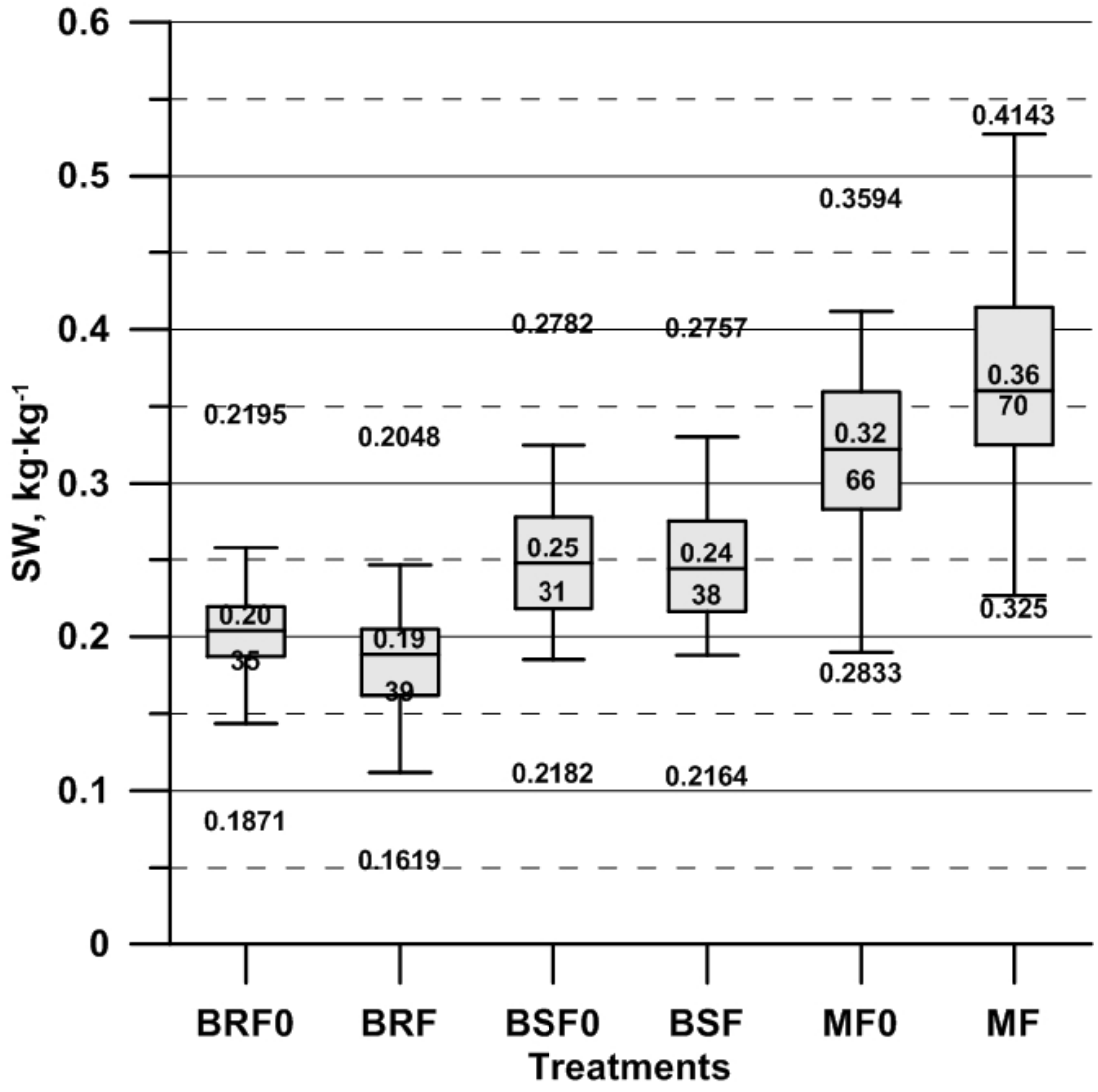
0.6
0.5
0.4
0.3
0.2
0.1
0
SW, kg·kg-1
0.4143
0.3594
0.2782
0.2757
0.2195
0.2048
0.36
70
0.32
66
0.25
31
0.24
38
0.20
35
0.19
39
0.325
0.2833
0.2182
0.2164
0.1871
0.1619
BRF0
BRF
BSF0
BSF
MF0
MF
Treatments

Figure 4b

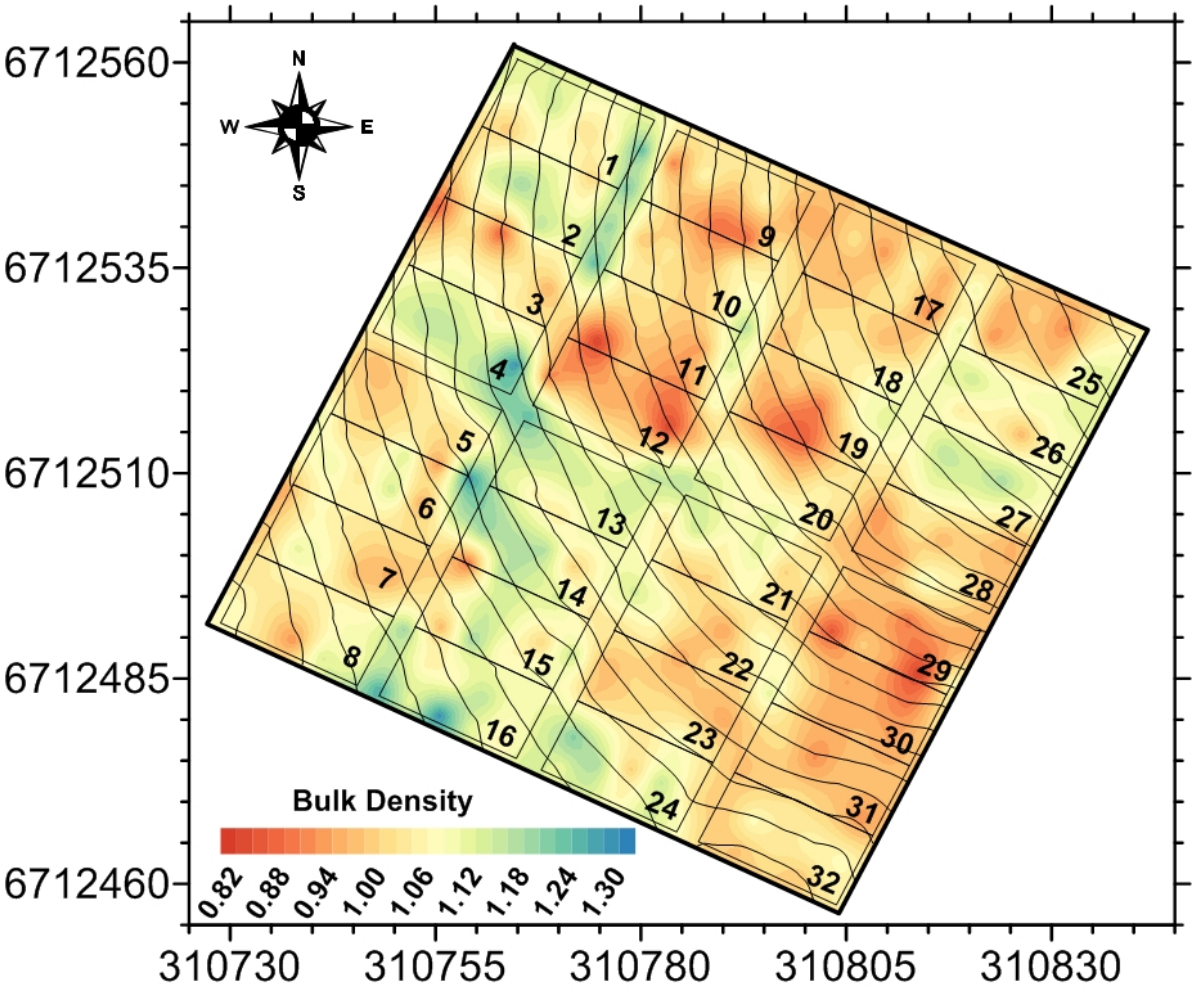
N
W
E
S
6712560
6712535
6712510
6712485
6712460
310730
310755
310780
310805
310830
1
2
3
4
5
6
7
8
9
10
11
12
13
14
15
16
17
18
19
20
21
22
23
24
25
26
27
28
29
30
31
32
Bulk Density
0.82
0.88
0.94
1.00
1.06
1.12
1.18
1.24
1.30

Figure 5a

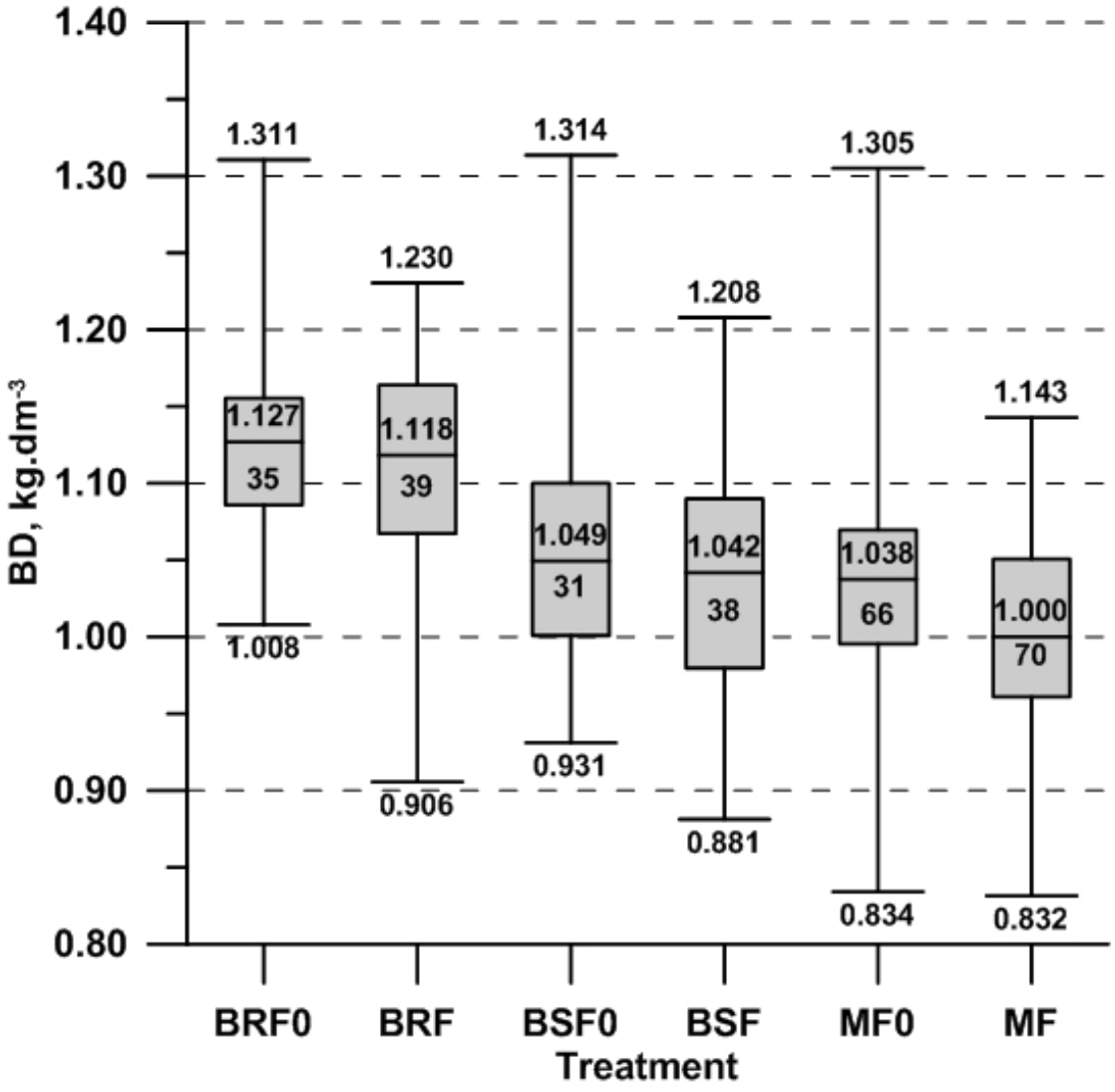
1.40
1.30
1.20
1.10
1.00
0.90
0.80
BD, kg.dm-3
1.311
1.127
35
1.008
1.230
1.118
39
0.906
1.314
1.049
31
0.931
1.208
1.042
38
0.881
1.305
1.038
66
0.834
1.143
1.000
70
0.832
BRF0
BRF
BSF0
BSF
MF0
MF
Treatment

Figure 5b

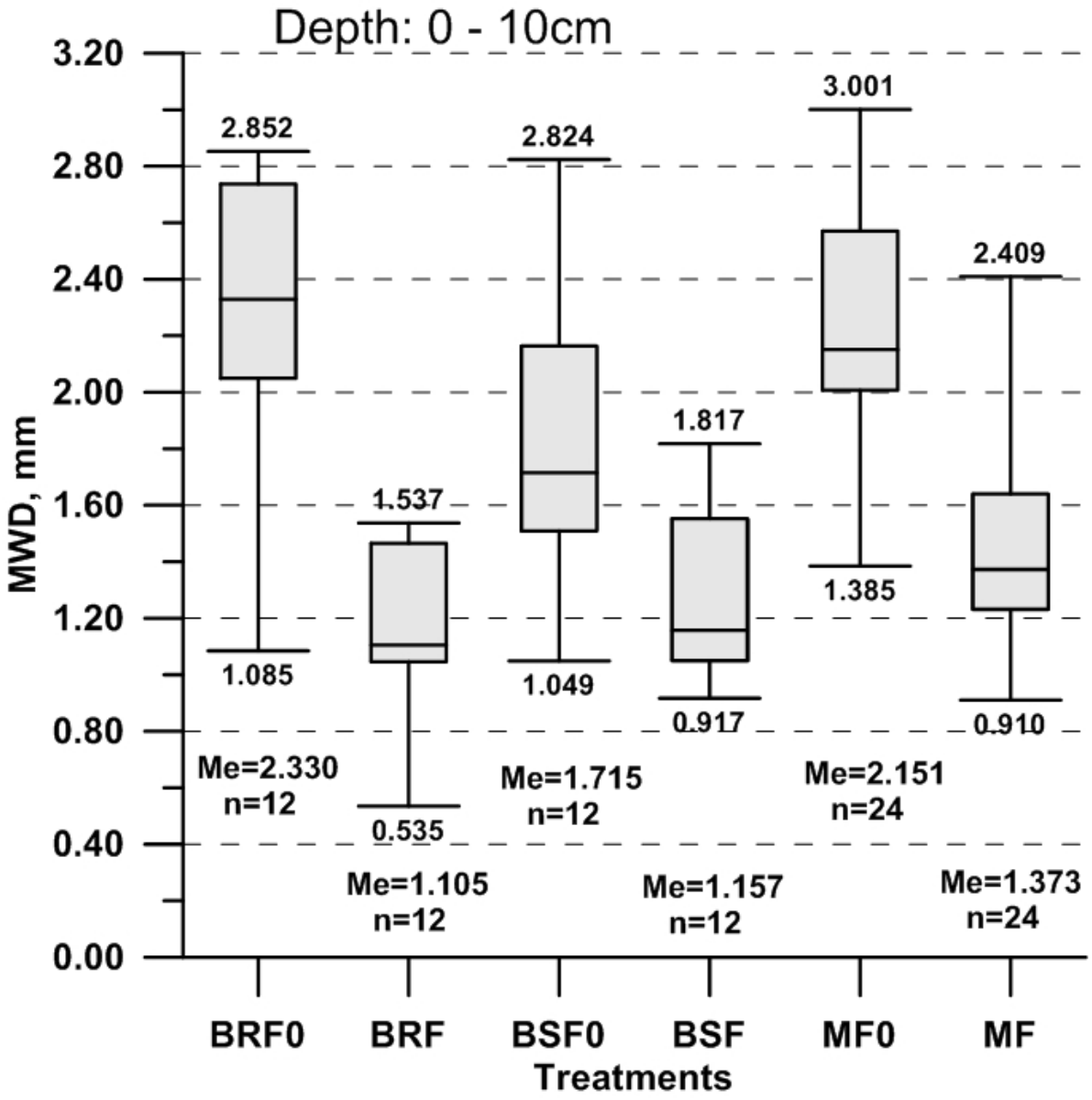
Depth: 0 - 10cm
MWD, mm
3.20
2.80
2.40
2.00
1.60
1.20
0.80
0.40
0.00
2.852
1.085
Me=2.330
n=12
1.537
0.535
Me=1.105
n=12
2.824
1.049
Me=1.715
n=12
1.817
0.917
Me=1.157
n=12
3.001
1.385
Me=2.151
n=24
2.409
0.910
Me=1.373
n=24
BRF0
BRF
BSF0
BSF
MF0
MF
Treatments

Figure 6a

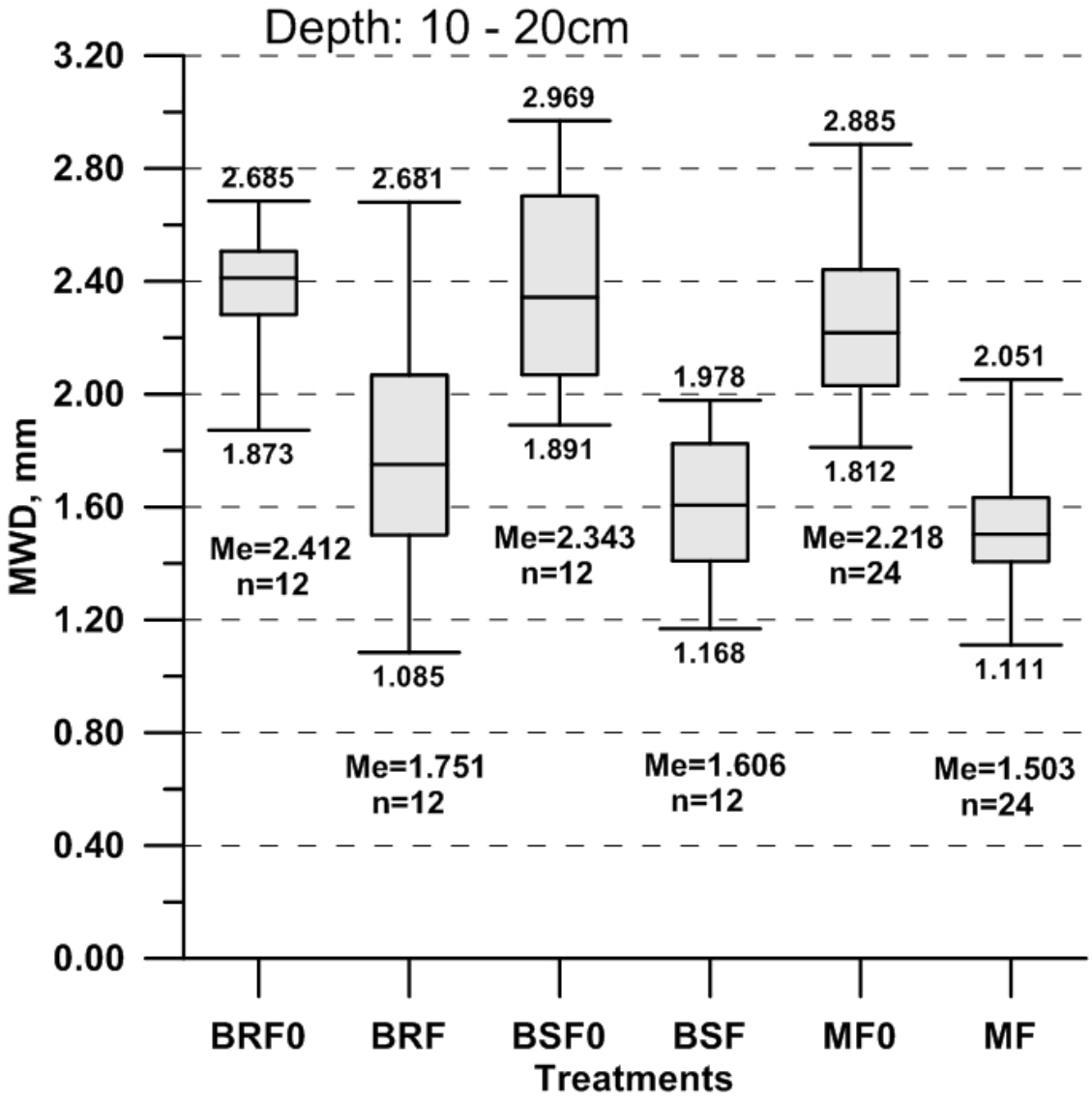

Figure 6b MWD 10 – 20cm

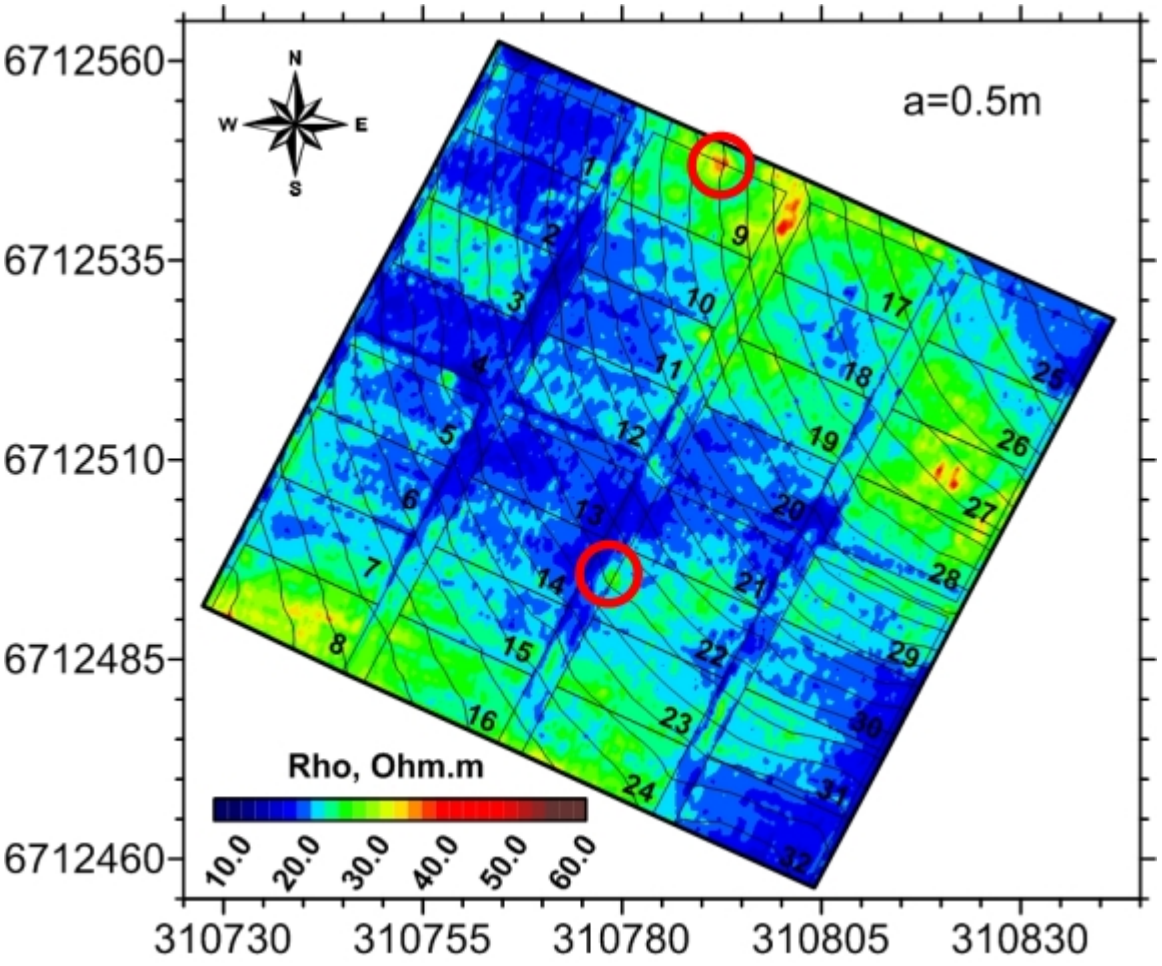
a=0.5m
N
W
E
S
Rho, Ohm.m
10.0
20.0
30.0
40.0
50.0
60.0
6712560
6712535
6712510
6712485
6712460
310730
310755
310780
310805
310830

Figure 7a

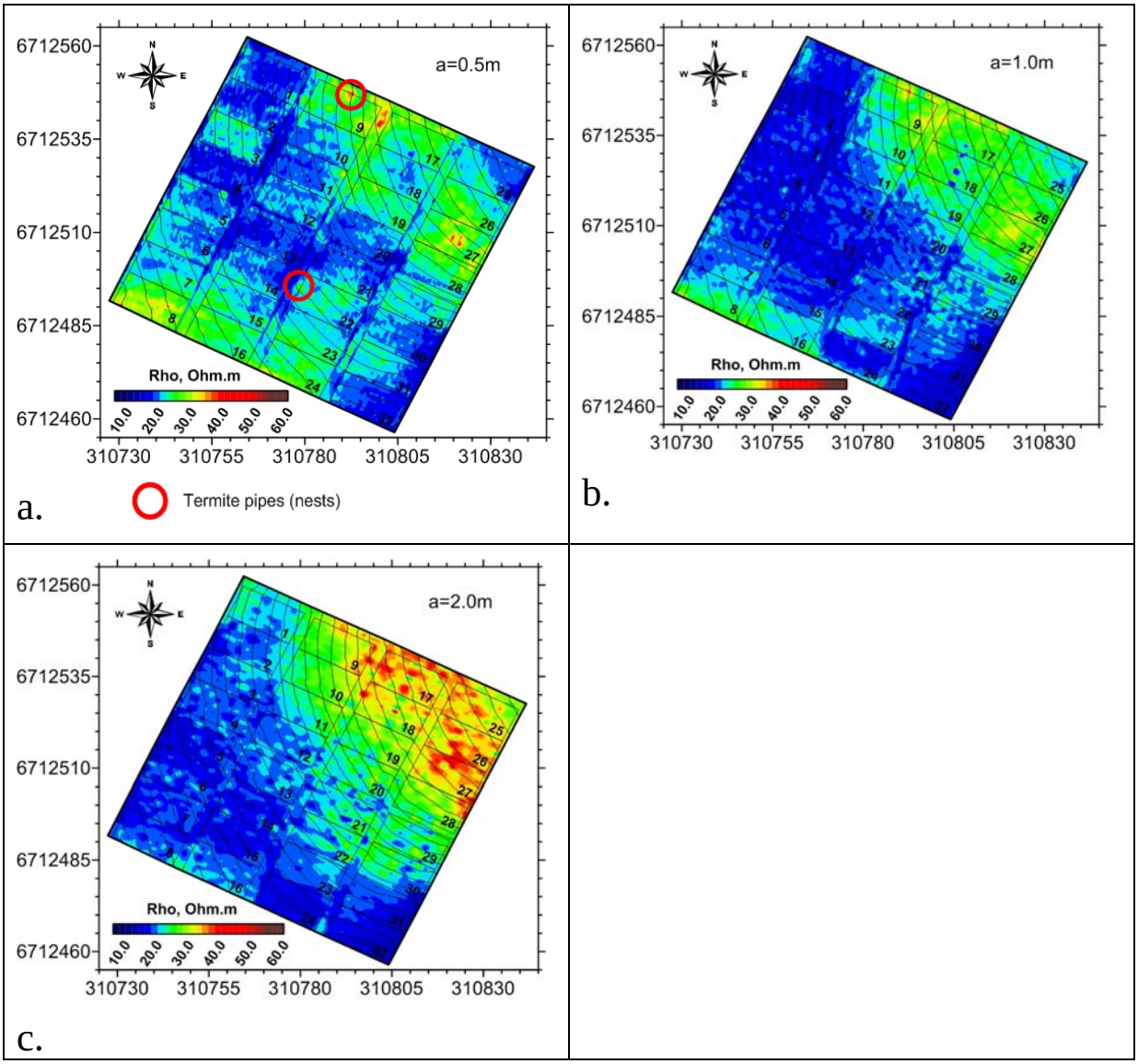

Figure 7a, b and c

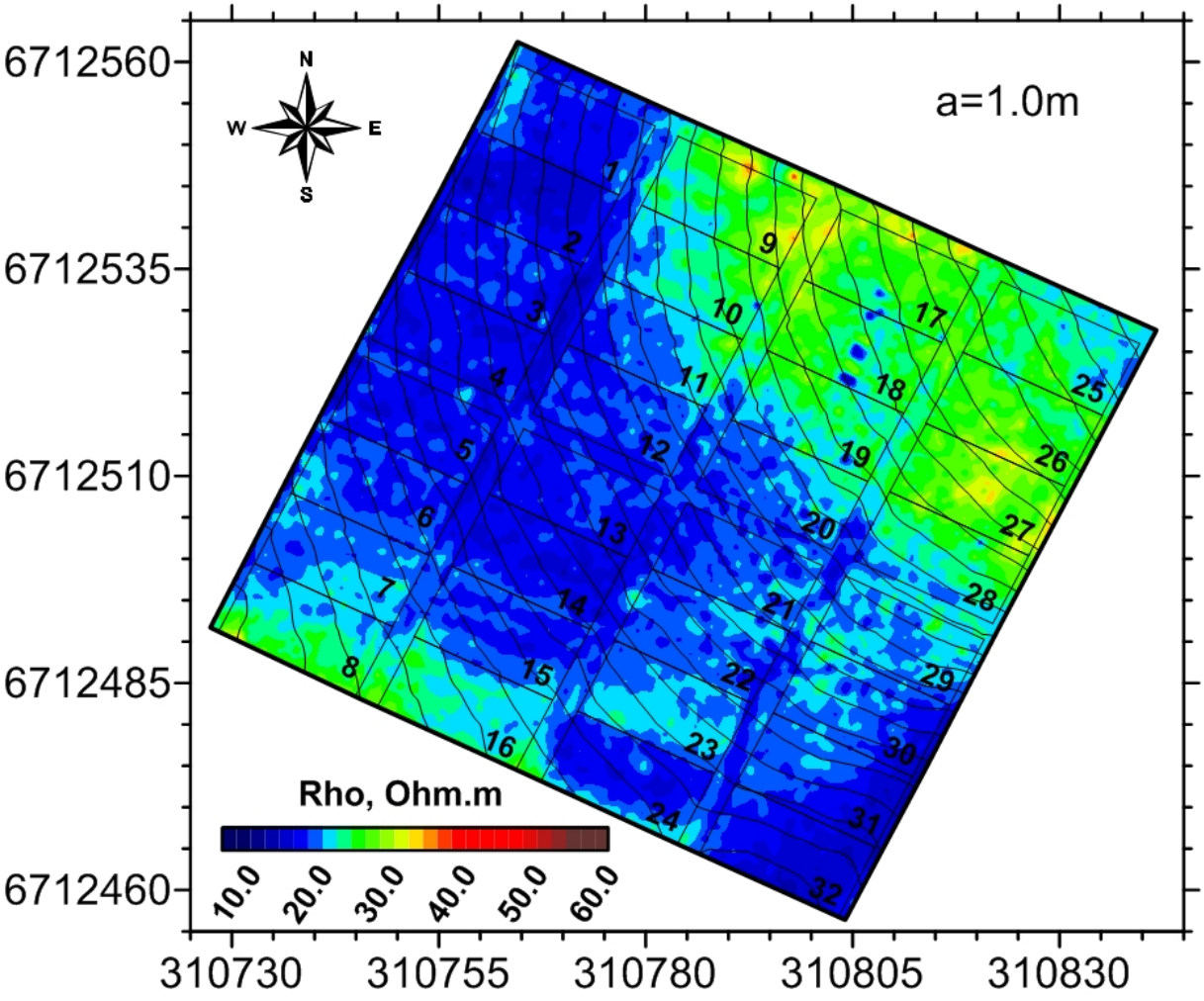
6712560
6712535
6712510
6712485
6712460
310730
310755
310780
310805
310830
N
W
E
S
a=1.0m
Rho, Ohm.m
10.0
20.0
30.0
40.0
50.0
60.0
1
2
3
4
5
6
7
8
9
10
11
12
13
14
15
16
17
18
19
20
21
22
23
24
25
26
27
28
29
30
31
32

Figure 7b,

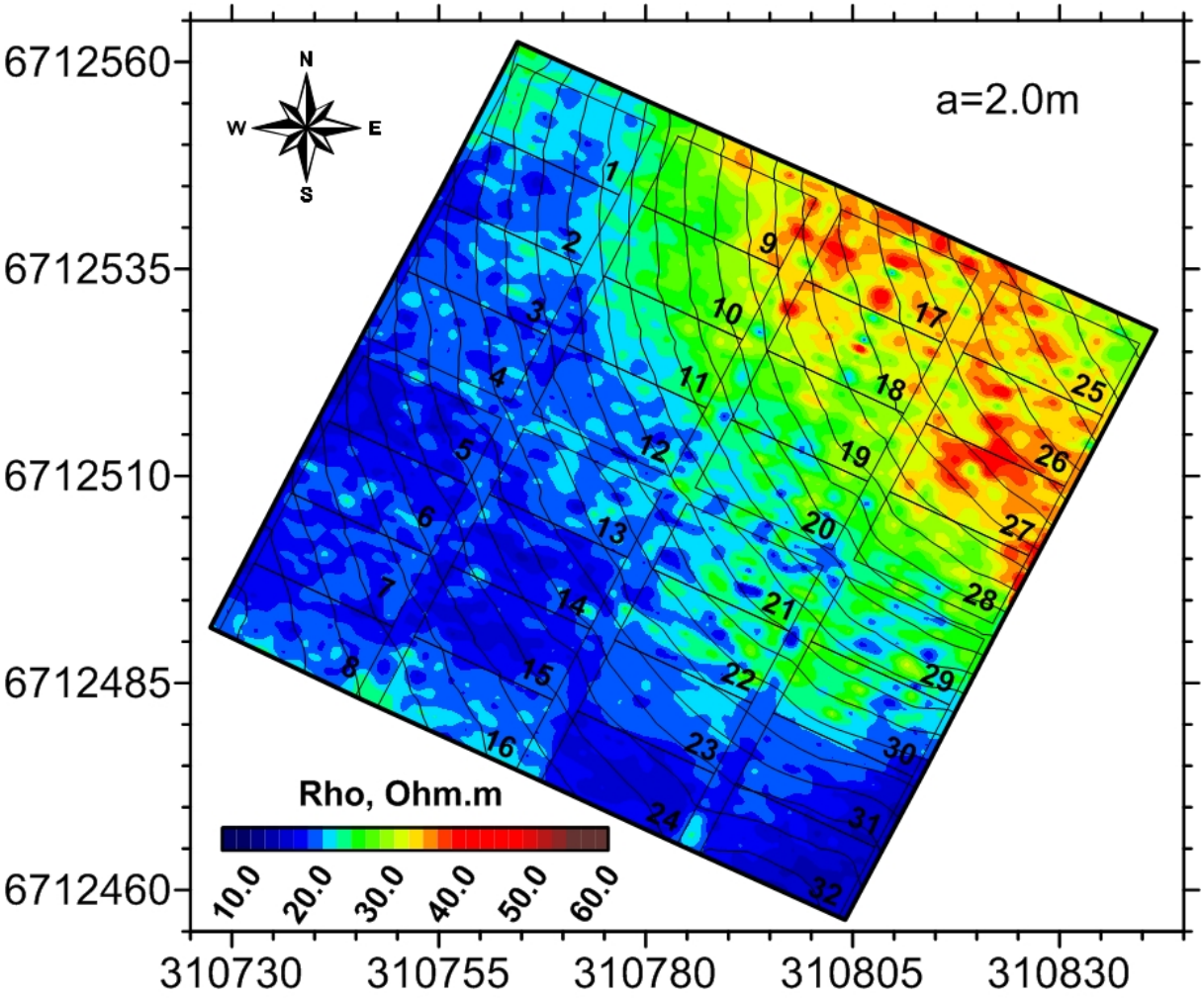
a=2.0m
N
W
E
S
Rho, Ohm.m
10.0
20.0
30.0
40.0
50.0
60.0
6712560
6712535
6712510
6712485
6712460
310730
310755
310780
310805
310830
1
2
3
4
5
6
7
8
9
10
11
12
13
14
15
16
17
18
19
20
21
22
23
24
25
26
27
28
29
30
31
32

Figure 7c

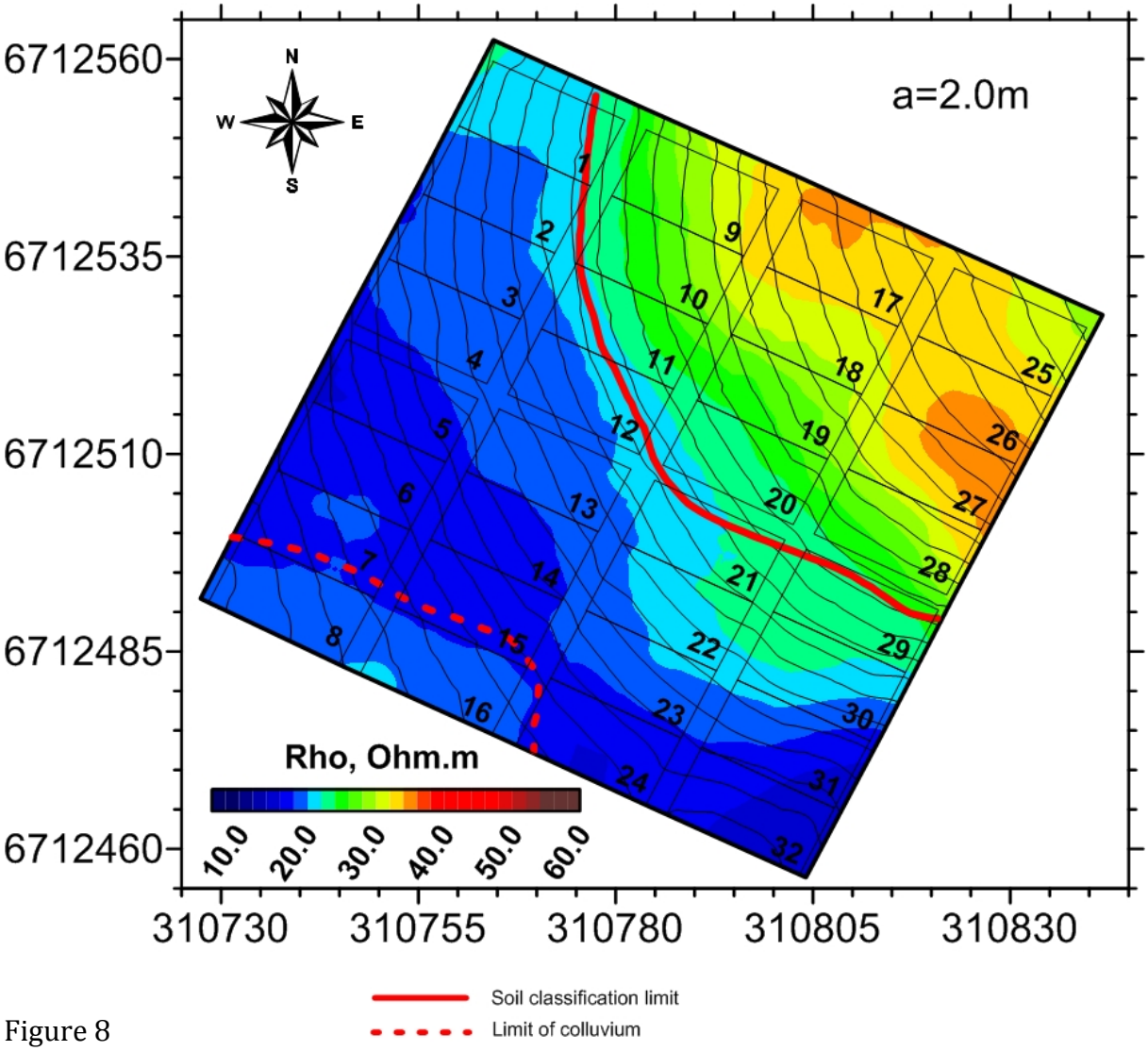
6712560
6712535
6712510
6712485
6712460
310730
310755
310780
310805
310830
N
W
E
S
a=2.0m
Rho, Ohm.m
10.0
20.0
30.0
40.0
50.0
60.0
Soil classification limit
Limit of colluvium

Figure 8